Pattern formation in Turing systems with space varying diffusion

José Luis Aragón

Centro de Física Aplicada y Tecnología Avanzada,
Universidad Nacional Autónoma de México.

Outline

After more than 50 years, the mechanism proposed by Alan Turing for the spontaneous generation of spatial patterns is still paradigmatic.

Turing's reaction-diffusion system:

$$\frac{\partial \mathbf{u}}{\partial t} = \mathbb{D}\nabla^2\mathbf{u} + \mathbf{F}(\mathbf{u}) \quad \text{in} \;\; \Omega,$$

$$\hat{\mathbf{n}} \cdot \nabla\mathbf{u} = 0 \quad \text{on} \;\; \partial\Omega.$$

- $\mathbf{u} = (u, v)^T$ are concentrations of chemicals that Turing called, generically, morphogens.
- $\mathbb{D}$ is the diagonal matrix of diffusion coefficients D_u and D_v.
- $\mathbf{F} = (f, g)^T$; $f(u, v)$, $g(u, v)$ are non-linear functions that determine the kinetics of the chemical reaction.

The Turing instability

A reaction-diffusion systems exhibits a diffusion-driven instability, also called Turing instability, if the homogeneous steady-state is stable to small perturbations in the absence of diffusion, but unstable to small spatial perturbations when diffusion is present.

A.M. Turing, "The chemical basis of morphogenesis " , *Philos. Trans. R. Soc. London B* **237** (1952) 37.

If $\mathbf{u}_0 = (u_0, v_0)$ is an steady state, *i.e.*, $\mathbf{F}(\mathbf{u}_0) = \mathbf{0}$, we consider $\mathbf{u} = \mathbf{u}_0 + \mathbf{v}$.

Linearizing about $\mathbf{u}_0$:

$$\frac{\partial \mathbf{v}}{\partial t} = \mathbb{J}\mathbf{v}, \tag{1}$$

where $\mathbb{J}$ is the Jacobian associated with the reaction kinetics $\mathbf{F}$, evaluated at $\mathbf{u}_0$.

The condition for stability in the absence of diffusion are:

$$\mathrm{Tr}(\mathbb{J}) < 0, \qquad \mathrm{Det}(\mathbb{J}) > 0.$$

The perturbation $\mathbf{v}$ is governed by the linear problem:

$$\frac{\partial \mathbf{v}}{\partial t} = \mathbb{D}\nabla^2 \mathbf{v} + \mathbb{J}\mathbf{v}.$$

Consider the spectral problem:

$$\nabla^2 \Phi = -\rho \Phi, \quad \text{in} \ \ \Omega,$$

$$\Phi = e^{i\mathbf{k}\cdot\mathbf{x}}, \quad \rho = k^2 = \|\mathbf{k}\|^2.$$

Therefore it seems reasonable to propose

$$\mathbf{v}(\mathbf{x}, t) = \sum_{k=0}^{\infty} \mathbf{C}_k(t) e^{i\mathbf{k}\cdot\mathbf{x}},$$

so that the evolution of the k-th Turing mode coefficient is

$$\frac{d\mathbf{C}_k}{dt} = \left(-k^2\mathbb{D} + \mathbb{J}\right)\mathbf{C}_k, \quad k = 0, 1, 2, \ldots.$$

Assuming $\mathbf{C}_k(t) = e^{\lambda_k t}\mathbf{c}_k$, we get

$$\left(\lambda_k \mathbb{I} + k^2\mathbb{D} - \mathbb{J}\right)\mathbf{c}_k = \mathbf{0}.$$

Nontrival solutions are obtained if

$$\lambda_k^2 - \operatorname{tr}\left(-k^2\mathbb{D} + \mathbb{J}\right)\lambda_k + \det\left(-k^2\mathbb{D} + \mathbb{J}\right) = 0.$$

$\mathrm{Re}(\lambda_k) > 0$ is obtained if an only if $\det(-k^2\mathbb{D} + \mathbb{J}) < 0$.

It is assumed that $\mathbb{D} = \operatorname{diag}[d, 1]$, were $d = D_u/D_v$. In this case

$$d_c = \frac{(\mathbb{J}_{11}\mathbb{J}_{22} - 2\mathbb{J}_{12}\mathbb{J}_{21}) - 2\sqrt{-\mathbb{J}_{12}\mathbb{J}_{21}\det(\mathbb{J})}}{\mathbb{J}_{22}^2}, \quad k_c^2 = \frac{\mathbb{J}_{11} + d_c\mathbb{J}_{22}}{2d_c}.$$

Linear analysis

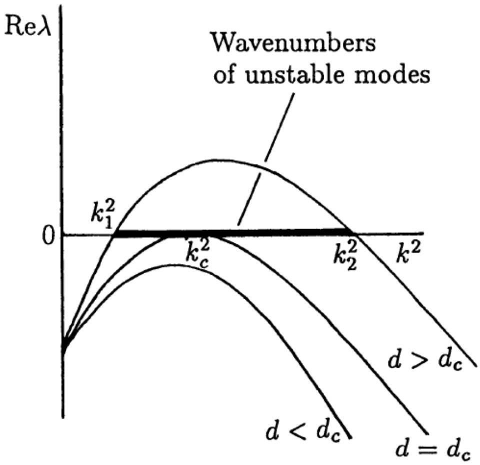

J.D. Murray, *Mathematical Biology II*.

Linear stability is useful to understand the basics of pattern formation:

- Diffusion is the key mechanism.
- Parameter values for the formation of the pattern can be determined.
- Patterns have a fixed wave-length $1/k_c$.

But, once the instability criterion is established, the determined dominant mode grows exponentially and is not valid at all times.

The long-time evolution of the pattern, and the determination of the type of pattern, should be studied by means of a nonlinear analysis.

For the nonlinear analysis it is taken into account that in a Turing bifurcation the linear instability is preceded by $\mathrm{Re}(\lambda_k) = 0$. Then, close to the bifurcation point the pattern evolves on a slow temporal scale as $e^{\lambda_k t}$, where $\lambda_k \approx 0$.

Therefore, the most useful approach is the multiple scales perturbation method, which has two key tricks:

- Introduces scaled space and time coordinates to capture the slow modulation of the pattern, treating these as separate variables in addition to the original variables that must be retained to describe the pattern state itself.
- Uses what are known as solvability conditions in the formal derivation.

- Close to the bifurcation point we assume

$$\mathbf{u} = \mathbf{u}_0 + \hat{\mathbf{u}}.$$

- Taylor series expansion of $\mathbf{F}(\mathbf{u})$, around $\mathbf{u}_0$, produces

$$\mathbf{F}(\mathbf{u}) = \mathbb{J}\hat{\mathbf{u}} + \mathbb{Q}(\hat{\mathbf{u}}, \hat{\mathbf{u}}) + \mathbb{C}(\hat{\mathbf{u}}, \hat{\mathbf{u}}, \hat{\mathbf{u}}) + \cdots ,$$

  where $\mathbb{J}$, $\mathbb{Q}$ and $\mathbb{C}$ are, respectively, the lineal quadratic and cubic terms evaluated at $\mathbf{u}_0$.
- A slow time scale is introduced:

$$T = \hat{w}t, \qquad \hat{w} = \epsilon w_1 + \epsilon^2 w_3 + \epsilon^3 w_2 \cdots ,$$

- Therefore the perturbation is governed by

$$\hat{w}\frac{\partial \hat{\mathbf{u}}}{\partial T} = \mathbb{D}\nabla^2\hat{\mathbf{u}} + \mathbb{J}\hat{\mathbf{u}} + \mathbb{Q}(\hat{\mathbf{u}}, \hat{\mathbf{u}}) + \mathbb{C}(\hat{\mathbf{u}}, \hat{\mathbf{u}}, \hat{\mathbf{u}}) + \cdots .$$

- Now, perturbations are assumed to be:

$$\mathbf{u} = \mathbf{u}_0 + \hat{\mathbf{u}} = \mathbf{u}_0 + \left(\epsilon\mathbf{u_1} + \epsilon^2\mathbf{u_2} + \epsilon^3\mathbf{u_3} + \cdots\right)$$
$$p = p_c + \hat{p} = p_c + \left(\epsilon p_1 + \epsilon^2 p_2 + \epsilon^3 p_3 + \cdots\right),$$

where p is a chosen parameter of the model.

- These perturbations are replaced in the above equation to get, to the various orders of ϵ, a hierarchy of linear differential equations:

- $$\begin{aligned}
O(\epsilon) &: \quad \mathcal{L}\mathbf{u}_1 = \mathbf{0},\\
O(\epsilon^2) &: \quad \mathcal{L}\mathbf{u}_2 = \mathbb{Q}(\mathbf{u}_1,\mathbf{u}_1) + p_1\mathbb{J}_p^c\mathbf{u}_1 - w_1\frac{\partial \mathbf{u}_1}{\partial T},\\
O(\epsilon^3) &: \quad \mathcal{L}\mathbf{u}_3 = \mathbb{Q}(\mathbf{u}_1,\mathbf{u}_2) + \mathbb{C}(\mathbf{u}_1,\mathbf{u}_1,\mathbf{u}_1) + p_2\mathbb{J}_p^c\mathbf{u}_1 + p_1\mathbb{J}_p^c\mathbf{u}_2 + \\
&\qquad p_1\mathbb{Q}^c(\mathbf{u}_1,\mathbf{u}_1) - w_1\frac{\partial \mathbf{u}_2}{\partial T} - w_2\frac{\partial \mathbf{u}_1}{\partial T},
\end{aligned}$$

  where $\mathcal{L} = (-\mathbb{J} - \mathbb{D}\nabla^2)$.

The analysis, which needs the $O(\epsilon^3)$, require the solutions of these linear system of equations. The algebra is horrendous but necessary. J.D. Murray, *Mathematical Biology II*.

- The solutions of $O(\epsilon)$ is proposed as linear combination of two spatial modes

$$\mathbf{u}_1 = \mathbf{V}^{(1)} a(T) e^{i\mathbf{k}_c \cdot \mathbf{x}} + \bar{\mathbf{V}}^{(1)} \bar{a}(T) e^{-i\mathbf{k}_c \cdot \mathbf{x}},$$

  and solving the equation of $O(\epsilon)$, $\mathbf{V}^{(1)}$ and $\bar{\mathbf{V}}^{(1)}$ are determined.
- The equation of $O(\epsilon^2)$ is solved to obtain $\mathbf{u}_2$, after applying the solvability condition (Fredholm alternative) to supress secular terms.
- With $\mathbf{u}_1$ and $\mathbf{u}_2$ at hand, the solvability condition is applied to the equation of $O(\epsilon^3)$ to finally obtain the equations of the amplitude functions $a(T)$ and $\bar{a}(T)$:

LACIAM CENTRO DE FÍSICA APLICADA Y TECNOLOGÍA AVANZADA

The Stuart-Landau equations:

$$\frac{d|a|^2}{dT} = \alpha|a|^4 + \beta|a|^2|\bar{a}|^2 + \theta|a|^2,$$
$$\frac{d|\bar{a}|^2}{dT} = \alpha|\bar{a}|^4 + \beta|a|^2|\bar{a}|^2 + \theta|\bar{a}|^2.$$

The explicit expressions of the coefficients α, β, and θ, result from this nonlinear analysis.

We don't really need to solve these equations.

A linear stability analysis of the Stuart-Landau equation, which has four equilibrium points, allows the identification of the type of spatial pattern to be formed:

Steady state	Conditions for linear stability	pattern
$\lvert a\rvert^2 = \lvert\bar{a}\rvert^2 = 0$	$\theta < 0$	None
$\lvert a\rvert^2 = 0, \lvert\bar{a}\rvert^2 = \frac{-\theta}{\alpha}$	$\theta > 0$ and $\frac{\beta}{\alpha} > 1$	Stripes
$\lvert a\rvert^2 = \frac{-\theta}{\alpha}, \lvert\bar{a}\rvert^2 = 0$	$\theta > 0$ and $\frac{\beta}{\alpha} > 1$	Stripes
$\lvert a\rvert^2 = \lvert\bar{a}\rvert^2 = \frac{\theta}{\alpha+\beta}$	$\theta > 0$ and $\alpha < -\lvert\beta\rvert < 0$	Spots

Weakly nonlinear analysis

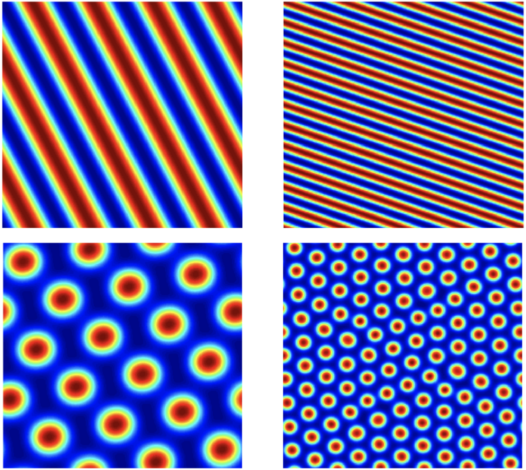

After 1952

At present I am not working on the problem at all, but on my mathematical theory of embryology, which I think I described to you at one time. This is yielding to treatment, and it will so far as I can see, give satisfactory explanations of -

i) Gastrulation.

ii) Polyogonally symmetrical structures, e.g., starfish, flowers.

iii) Leaf arrangement, in particular the way the Fibonacci series (0, 1, 1 = 2, 3, 5, 8, 13,.......) comes to be involved.

iv) Colour patterns on animals, e.g., stripes, spots and dappling.

v) Patterns on nearly spherical structures such as some Radiolaria, but this is more difficult and doubtful.

The Turing Digital Archive: `https://turingarchive.kings.cam.ac.uk`.

Turing's work on morphogenesis remained largely unknown until more that 25 years when the existence of morphogen gradients was pointed out: C. Nüsslein-Volhard, E. Wieschaus, *Nature* **287** (1980) 795-801.

It was found that the Turing instability occurs in a great variety of other systems as well:

- Taylor vortex flow:
  E. Koschmeider, *Order and fluctuation in in equilibrium and nonequilibrium statistical mechanics* Wiley (1981).
- Dynamic solidification:
  J. Langer, *Rev. Mod. Phys.* **52** (1980) 1-28.
- Laser Physics:
  A. Newell, J. Maloney, *Nonlinear optics*, Addison-Wesley (1992).

Most popular kinetics

Chemical kinetics	Name	Application
$F(u,v) = \mu u(1 - u/K)$	Fisher	Bacteria population
$F(u,v) = au - buv$ $G(u,v) = -cu + duv$	Lotka-Volterra	Prey-predator dynamics
$F(u,v) = \rho_u - \mu_u u + \rho u^2/v$ $G(u,v) = \rho_v - \mu_v v + \rho u^2$	Gierer-Meinhardt	General
$F(u,v) = f(1-u) - uv^2$ $G(u,v) = bu - u^2 v$	Gray-Scott	Cell glycolysis
$F(u,v,w) = [\varepsilon(qv - uv + u(1-u))]^{-1}$ $G(u,v,w) = [\varepsilon'(-qv - uv + fw)]^{-1}$ $H(u,v,w) = u - v$	Oregonator	Belusov-Zhabotinsky
$F(u,v) = a - (b+1)u + u^2 v$ $G(u,v) = bu - u^2 v$	Brusselator	Auto-catalytic reactions
$F(u,v) = a - u - 4uv/\left(1+u^2\right)$ $G(u,v) = \delta\left(u - uv/\left(1+u^2\right)\right)$	Lengyel-Epstein	Chlorine-iodide-malonic acid reaction
$F(u,v) = \gamma\left(a - u + u^2 v\right)$ $G(u,v) = \gamma\left(b - u^2 v\right)$	Shnakenberg	Oregonator simplified
$F(u,v) = -v + u + u^3$ $G(u,v) = \varepsilon(u - \alpha v - \beta)$	Fitzhugh-Nagumo	Pulse propagation in nerve membrane

The BVAM model

The BVAM model was proposed in 1999 as a general purposes, yet simple, model, which presents a rich bifurcation structure and constitutes a versatile system for modeling biological phenomena.

The BVAM model

$$\begin{aligned} \frac{\partial u}{\partial t} &= D\,\nabla^2 u + \eta\left(u + av - cuv - uv^2\right), \\ \frac{\partial v}{\partial t} &= \nabla^2 u + \eta\left(bv + hu + cuv + uv^2\right). \end{aligned}$$

C. Varea, R.A. Barrio, J.L. Aragón, P.K. Maini, *Bull. Math. Biol.* **61** (1999) 483.

Coupling reaction-diffusion equations

One way to generate a larger variety of patterns is by coupling two reaction-diffusion systems:

$$\begin{aligned} \frac{\partial \mathbf{u}}{\partial t} &= \mathbb{D}_{\mathbf{u}} \nabla^2 \mathbf{u} + \mathbf{F}(\mathbf{u}) + \mathbb{K}_{\mathbf{u}}(\mathbf{u}, \mathbf{v}), \\ \frac{\partial \mathbf{v}}{\partial t} &= \mathbb{D}_{\mathbf{v}} \nabla^2 \mathbf{v} + \mathbf{G}(\mathbf{v}) + \mathbb{K}_{\mathbf{v}}(\mathbf{u}, \mathbf{v}), \end{aligned}$$

where $\mathbb{K}_{\mathbf{u}}$ and $\mathbb{K}_{\mathbf{v}}$ are coupling functions:

$$\mathbb{K}_{\mathbf{u}} = \begin{pmatrix} p(u_1 - v_1) \\ q(u_2 - v_2) \end{pmatrix}, \quad \mathbb{K}_{\mathbf{v}} = \begin{pmatrix} p(v_1 - u_1) \\ q(v_2 - u_2) \end{pmatrix}.$$

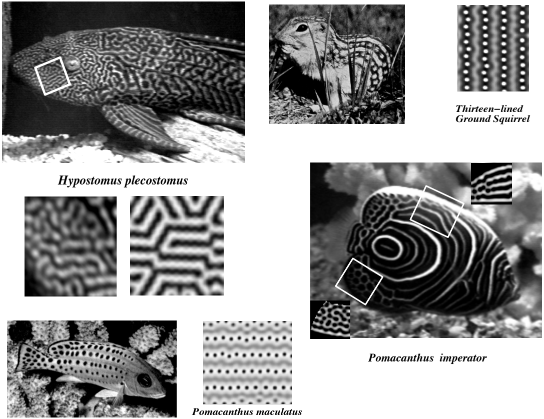

Aragón, Varea & Barrio, *FORMA* **13** (1998) 213.

Non-trivial domains

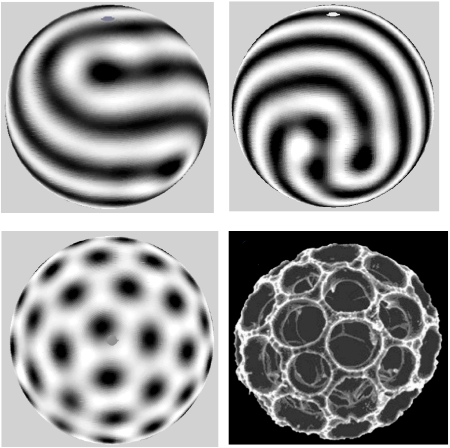

Varea, Aragón, Barrio *Phys. Rev. E* **60** (1999) 4588.

Modulation instability

The BVAM model can be transformed onto one equation that resembles the one used to study localized structures in nonlinear optics.

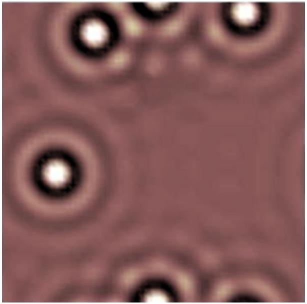

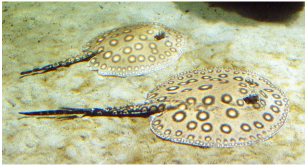

Wooley, Baker, Maini, Aragón, Barrio, *Phys. Rev. E* **82** (2010) 051929.

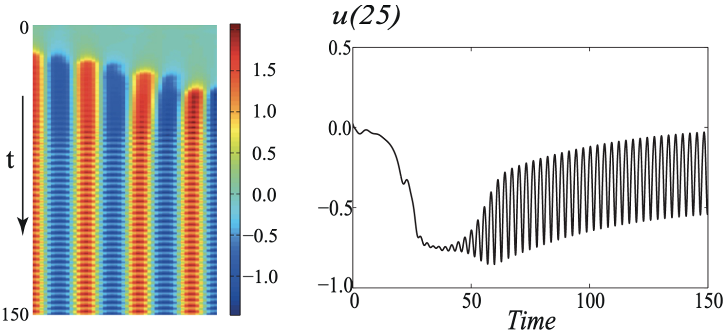

Aragón, Barrio, Wooley, Baker, Maini, *Phys. Rev. E* **86** (2012) 026201.

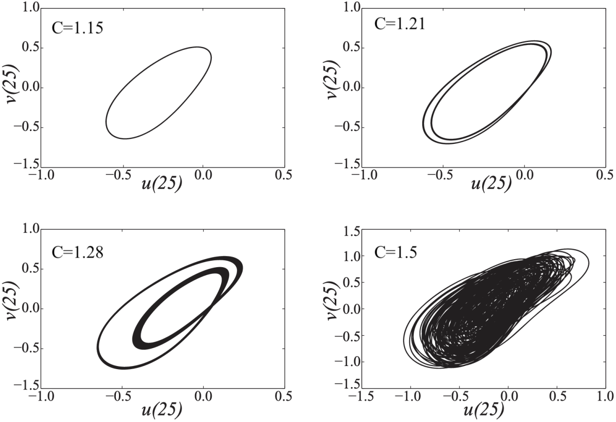

Aragón, Barrio, Wooley, Baker, Maini, *Phys. Rev. E* **86** (2012) 026201.

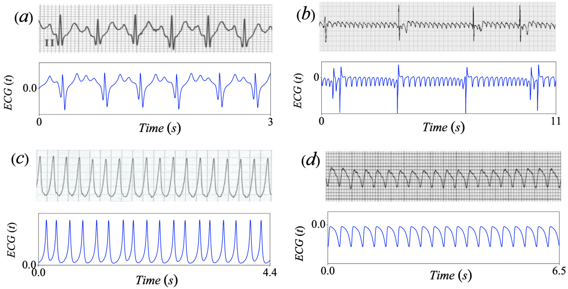

Figure 6. Comparison of ECG plots obtained from experimental observations (top panels) and the reduced system (3) (bottom panels). (**a**) Sinus tachycardia[44], (**b**) Atrial flutter[42], (**c**) Ventricular tachycardia[45] and (**d**) Ventricular flutter[46].

Generation of ECG signals from a reaction-diffusion model spatially discretized

M. A. Quiroz-Juárez, O. Jiménez-Ramírez, R. Vázquez-Medina, V. Breña-Medina, J. L. Aragón & R. A. Barrio

Scientific Reports **9**, Article number: 19000 (2019) | Cite this article

Phyllotaxis

The arrangement of lateral organs (such as leaves, scales, florets) on a plant surface.

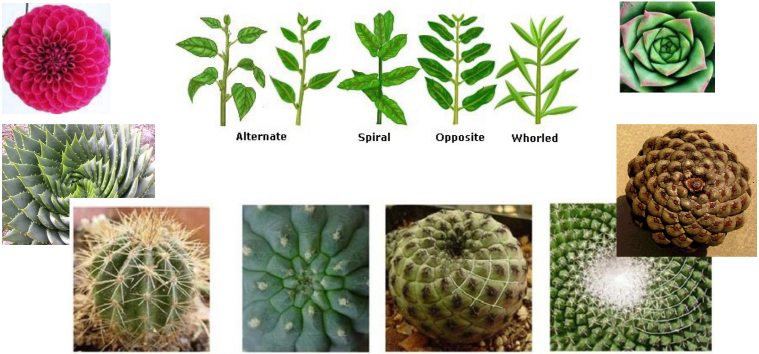

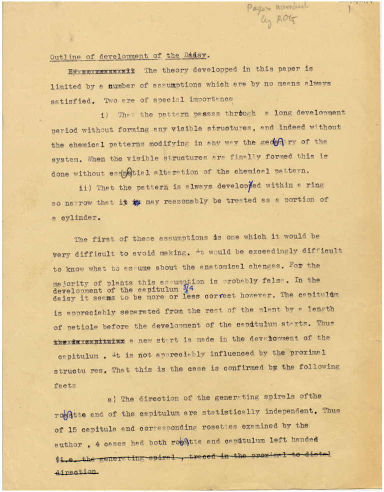
Pages numbered by AOG

Outline of development of the Daisy.

The theory developped in this paper is limited by a number of assumptions which are by no means always satisfied. Two are of special importance

i) That the pattern passes through a long development period without forming any visible structures, and indeed without the chemical patterns modifying in any way the geometry of the system. When the visible structures are finally formed this is done without essential alteration of the chemical pattern.

ii) That the pattern is always developed within a ring so narrow that it may reasonably be treated as a portion of a cylinder.

The first of these assumptions is one which it would be very difficult to avoid making. It would be exceedingly difficult to know what to assume about the anatomical changes. For the majority of plants this assumption is probably false. In the development of the capitulum of a daisy it seems to be more or less correct however. The capitulum is appreciably separated from the rest of the plant by a length of petiole before the development of the capitulum starts. Thus a new start is made in the development of the capitulum. It is not appreciably influenced by the proximal structures. That this is the case is confirmed by the following facts

a) The direction of the generating spirals of the rosette and of the capitulum are statistically independent. Thus of 15 capitula and corresponding rosettes examined by the author, 4 cases had both rosette and capitulum left handed ~~(i.e. the generating spiral, traced in the proximal to distal direction~~

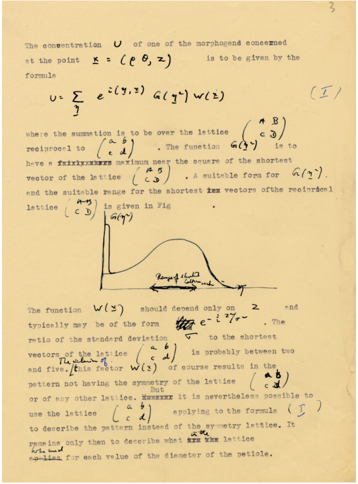
3

The concentration U of one of the morphogens concerned at the point $x = (\rho\, \theta, z)$ is to be given by the formula

$$U = \sum_{\eta} e^{i(\eta, x)} G(\eta^2) W(z) \qquad (I)$$

where the summation is to be over the lattice $\begin{pmatrix} A & B \\ C & D \end{pmatrix}$ reciprocal to $\begin{pmatrix} a & b \\ c & d \end{pmatrix}$. The function $G(\eta^2)$ is to have a maximum near the square of the shortest vector of the lattice $\begin{pmatrix} A & B \\ C & D \end{pmatrix}$. A suitable form for $G(\eta^2)$ and the suitable range for the shortest vectors of the reciprocal lattice $\begin{pmatrix} A & B \\ C & D \end{pmatrix}$ is given in Fig .

The function $W(z)$ should depend only on z and typically may be of the form e^{-z^2/σ^2}. The ratio of the standard deviation σ to the shortest vectors of the lattice $\begin{pmatrix} a & b \\ c & d \end{pmatrix}$ is probably between two and five. The value of this factor $W(z)$ of course results in the pattern not having the symmetry of the lattice $\begin{pmatrix} a & b \\ c & d \end{pmatrix}$ or of any other lattice. But it is nevertheless possible to use the lattice $\begin{pmatrix} a & b \\ c & d \end{pmatrix}$ applying to the formula (I) to describe the pattern instead of the symmetry lattice. It remains only then to describe what the lattice to be used applies for each value of the diameter of the petiole.

The Turing Digital Archive: `https://turingarchive.kings.cam.ac.uk`.

Phyllotaxis

Regulation of phyllotaxis by polar auxin transport

Didier Reinhardt, Eva-Rachele Pesce, Pia Stieger, Therese Mandel, Kurt Baltensperger, Malcolm Bennett, Jan Traas, Jiří Friml & Cris Kuhlemeier

Nature **426**, 255–260 (2003) | Cite this article

10k Accesses | **1087** Citations | **13** Altmetric | Metrics

Abstract

The regular arrangement of leaves around a plant's stem, called phyllotaxis, has for centuries attracted the attention of philosophers, mathematicians and natural scientists; however, to date, studies of phyllotaxis have been largely theoretical. Leaves and flowers are formed from the shoot apical meristem, triggered by the plant hormone auxin. Auxin is transported through plant tissues by specific cellular influx and efflux carrier proteins. Here we show that proteins involved in auxin transport regulate phyllotaxis. Our data indicate that auxin is transported upwards into the meristem through the epidermis and the outermost meristem cell layer. Existing leaf primordia act as sinks, redistributing auxin and creating its heterogeneous distribution in the meristem. Auxin accumulation occurs only at certain minimal distances from existing primordia, defining the position of future primordia. This model for phyllotaxis accounts for its reiterative nature, as well as its regularity and stability.

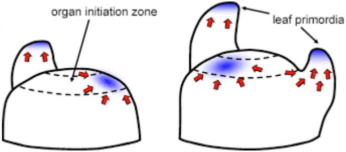

An auxin-driven polarized transport model for phyllotaxis

Henrik Jönsson*†, Marcus G. Heisler†‡, Bruce E. Shapiro§, Elliot M. Meyerowitz‡¶, and Eric Mjolsness¶‖

*Computational Biology and Biological Physics Group, Department of Theoretical Physics, Lund University, S-221 00 Lund, Sweden; ‡Division of Biology and §Biological Network Modeling Center, California Institute of Technology, Pasadena, CA 91125; and ‖Institute of Genomics and Bioinformatics and Department of Computer Science, University of California, Irvine, CA 92697

Flower Development as an Interplay between Dynamical Physical Fields and Genetic Networks

Rafael Ángel Barrio[1]*, Aurora Hernández-Machado[2], C. Varea[1], José Roberto Romero-Arias[1], Elena Álvarez-Buylla[3]*

1 Departamento de Física Qumica, Instituto de Física, Universidad Nacional Autónoma de México, México D.F., Mexico, 2 Department of Structure and Constituents of Matter, Facultat de Física, Universitat de Barcelona, Barcelona, Spain, 3 Instituto de Ecología, Universidad Nacional Autónoma de México, México D.F., Mexico

Super multi-armed and segmented spiral pattern in a reaction-diffusion model

JIAN GAO and CHANGGUI GU
Department of Systems Science, University of Shanghai for Science and Technology, Shanghai 200093, P. R. China
Corresponding author: Changgui Gu (e-mail: gu_changgui@163.com).

A plausible model of phyllotaxis

Richard S. Smith*†, Soazig Guyomarc'h†‡, Therese Mandel‡, Didier Reinhardt‡§, Cris Kuhlemeier‡, and Przemyslaw Prusinkiewicz*¶

*Department of Computer Science, University of Calgary, 2500 University Drive NW, Calgary, AB, Canada T2N 1N4; and ‡Institute of Plant Sciences, University of Berne, CH-3013 Berne, Switzerland

The Role of Mechanical Forces in Plant Morphogenesis

Vincent Mirabet, Pradeep Das, Arezki Boudaoud, and Olivier Hamant

INRA, CNRS, ENS, Université de Lyon, 46 Allée d'Italie, 69364 Lyon Cedex 07, France; email: olivier.hamant@ens-lyon.fr

Elastic Domains Regulate Growth and Organogenesis in the Plant Shoot Apical Meristem

Daniel Kierzkowski,[1]* Naomi Nakayama,[1]* Anne-Lise Routier-Kierzkowska,[1]* Alain Weber,[1]* Emmanuelle Bayer,[2] Martine Schorderet,[3] Didier Reinhardt,[3] Cris Kuhlemeier,[1] Richard S. Smith[1]†

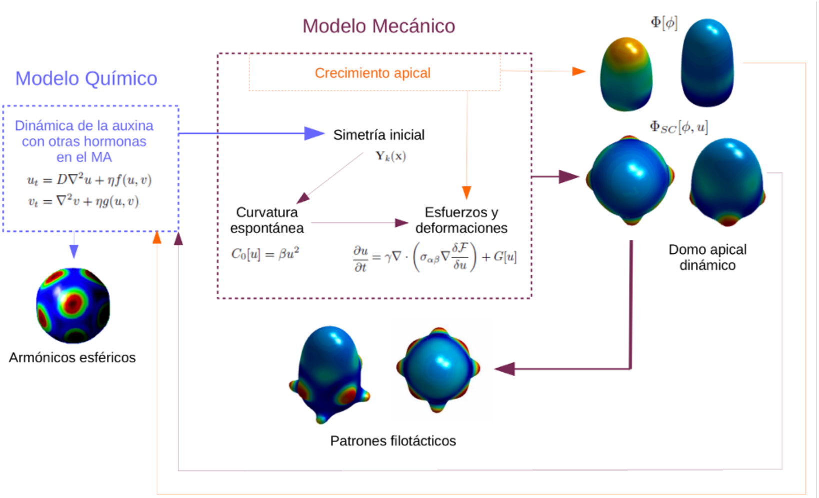
Modelo Mecánico
Crecimiento apical
$\Phi[\phi]$
Modelo Químico
Dinámica de la auxina con otras hormonas en el MA
$u_t = D\nabla^2 u + \eta f(u,v)$
$v_t = \nabla^2 v + \eta g(u,v)$
Simetría inicial
$\mathbf{Y}_k(\mathbf{x})$
$\Phi_{SC}[\phi, u]$
Curvatura espontánea
$C_0[u] = \beta u^2$
Esfuerzos y deformaciones
$\frac{\partial u}{\partial t} = \gamma \nabla \cdot \left(\sigma_{\alpha\beta} \nabla \frac{\delta \mathcal{F}}{\delta u} \right) + G[u]$
Domo apical dinámico
Armónicos esféricos
Patrones filotácticos

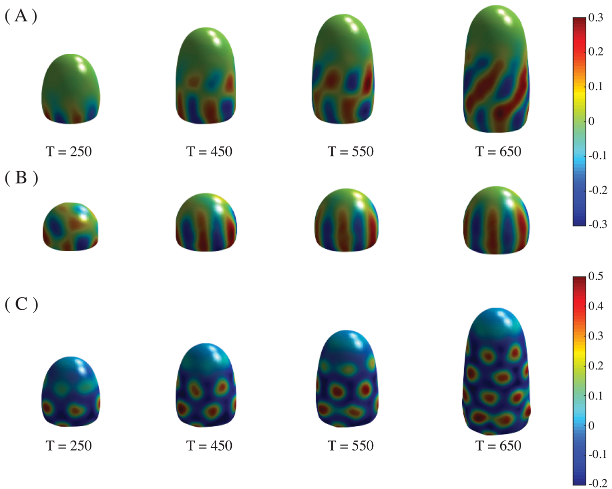

Rueda, Romero, Aragón, Barrio, *Plos One* **13** (2018) e0201746.

Space-dependent diffusion coefficient

The general problem:

$$\frac{\partial \mathbf{u}}{\partial t} = \mathbb{D}\nabla \cdot (\mathcal{D}(\mathbf{x})\nabla \mathbf{u}) + \eta \mathbf{F}(\mathbf{u}) \quad \text{in} \;\; \Omega,$$

$$\mathbf{n} \cdot (\mathcal{D}(\mathbf{x})\nabla \mathbf{u}) = 0 \quad \text{on} \;\; \partial\Omega,$$

where $\mathbb{D} = \mathrm{diag}[d, 1]$ already considered, $\mathcal{D}(\mathbf{x})$ is a function that describes the spatial variation of the diffusion rate, and η is a non-dimensional coefficient related to the size of the space domain

Space-dependent diffusion coefficient (1D)

- Maini, Benson, Sherrat, *IMA J. Math. Appl. Med. Biol.* **9** (1992) 197.
  Wei, Winter, *J. Nonlinear Sci.* **19** (2009) 301.

$$D(x) = \begin{cases} D^+ & 0 \leq x < \xi \\ D^- & \xi < x \leq 1 \end{cases}$$

- Benson, Maini, Sherrat, *J. Math. Biol.* **37** (1998) 381.

$$D(x) = D + \eta x^2$$

- Chacón-Acosta, Núñez-López, Pineda *J. Chem. Phys.* **152** (2020) 024101.

$$\frac{\partial p}{\partial t} = D_0 \frac{\partial}{\partial x}\left[w(x)\frac{\partial}{\partial x}\left(\frac{p}{w(x)}\right)\right] + F.$$

The general problem:

$$\frac{\partial \mathbf{u}}{\partial t} = \mathbb{D}\nabla \cdot (\mathcal{D}(\mathbf{x})\nabla \mathbf{u}) + \eta \mathbf{F}(\mathbf{u}) \quad \text{in} \;\; \Omega,$$

$$\mathbf{n} \cdot (\mathcal{D}(\mathbf{x})\nabla \mathbf{u}) = 0 \quad \text{on} \;\; \partial\Omega,$$

where $\mathbb{D} = \mathrm{diag}[d, 1]$ already considered, $\mathcal{D}(\mathbf{x})$ is a function that describes the spatial variation of the diffusion rate, and η is a non-dimensional coefficient related to the size of the space domain

As before, the perturbation $\mathbf{v}$, around the steady state $\mathbf{u}_0$, is governed by the linear problem:

$$\frac{\partial \mathbf{v}}{\partial t} = D\nabla \cdot (\mathcal{D}(\mathbf{x})\nabla \mathbf{v}) + \eta J\mathbf{v}, \quad \text{in } \Omega$$

$$\mathbf{n} \cdot (\mathcal{D}(\mathbf{x})\nabla \mathbf{v}) = 0, \quad \text{on } \partial\Omega.$$

Consider the spectral problem:

$$\nabla \cdot (\mathcal{D}(\mathbf{x})\nabla \Phi) = -\rho\, \Phi, \quad \text{in } \Omega$$

$$\mathbf{n} \cdot (\mathcal{D}(\mathbf{x})\nabla \Phi) = 0, \quad \text{on } \partial\Omega.$$

When solutions exist, there is an infinite but countable set of real eigenvalues ρ_i, and the corresponding set of eigenfunctions $\Phi_0, \Phi_1, \ldots$, form a complete basis functions on Ω satisfying the given boundary conditions.

Therefore it seems reasonable to propose

$$\mathbf{v}(\mathbf{x},t)=\sum_{n=0}^{\infty}\mathbf{C}_n(t)\Phi_n(\mathbf{x}),$$

By following the procedure already described, we obtain the dispersion relation:

$$\lambda_k^2-\mathrm{tr}\left(-\rho_k\mathbb{D}+\eta\mathbb{J}\right)\lambda_k+\det\left(-\rho_k\mathbb{D}+\eta\mathbb{J}\right)=0,$$

from which we obtain:

$$d_c=\frac{(\mathbb{J}_{11}\mathbb{J}_{22}-2\mathbb{J}_{12}\mathbb{J}_{21})-2\sqrt{-\mathbb{J}_{12}\mathbb{J}_{21}\det(\mathbb{J})}}{\mathbb{J}_{22}^2},\quad \rho_c=\eta\frac{\mathbb{J}_{11}+d_c\mathbb{J}_{22}}{2d_c}.$$

The linear problem is the same but ρ_k must be known.

1D

Consider the $1D$ BVAM model in the space domain $\Omega = [-1, 1]$:

$$\frac{\partial u}{\partial t} = d\,\frac{\partial}{\partial x}\left(\mathcal{D}(x)\frac{\partial u}{\partial x}\right) + \eta\left(u + av - cuv - uv^2\right)$$

$$\frac{\partial v}{\partial t} = \frac{\partial}{\partial x}\left(\mathcal{D}(x)\frac{\partial v}{\partial x}\right) + \eta\left(bv + hu + cuv + uv^2\right)$$

$$\mathcal{D}(x)\frac{\partial u}{\partial x} = 0, \quad \mathcal{D}(x)\frac{\partial v}{\partial x} = 0 \qquad \text{at} \;\; x = -1, 1.$$

This system has three steady states, including $(u_0, v_0) = (0, 0)$.

Associated (Sturm-Liouville) spectral problem:

$$\frac{d}{dx}\left(\mathcal{D}(x)\frac{d\Phi}{dx}\right) = -\rho\Phi, \quad \text{in } \Omega = [-1, 1]$$

$$\mathcal{D}(x)\frac{d\Phi}{dx} = 0, \quad \text{at } x = -1, 1.$$

$\mathcal{D}(x) = 1$ in this case $\Phi_k = \cos(kx)$, $\rho_k = k^2 = (n\pi)^2$, and the linear analysis yields:

$$d_c = \frac{1}{2\sqrt{ah(ah-b)} - 2ah + b},$$

$$k_c^2 = \eta^2\left(\sqrt{ah(ah-b)} - ah + b\right).$$

$\mathcal{D}(x) = 1 - x^2$ in this case $\Phi_k = P_k(x)$, the Legendre polynomials of degree $k \in \mathbb{N}$, $\rho_k = k(k+1)$, and the linear analysis yields the same d_c but:

$$k_c(k_c+1) = \eta^2 \left(\sqrt{ah(ah-b)} - ah + b \right).$$

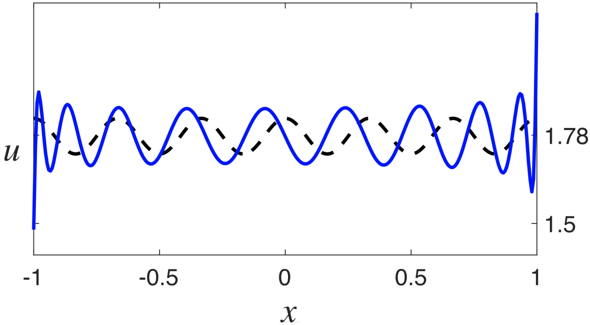

$a = 3$, $b = -2$, $h = -1$, $c = 0.95$, $d_c = 0.133975$, $\eta = 10.9808$,

$k_c = 18.1501$ (homogeneous), $k_c = 18$ (Legendre).

2D

In the space domain $\Omega = [-1,1] \times [-1,1]$

$$\frac{\partial u}{\partial t} = d\, \nabla \cdot (\mathcal{D}_{11}(\mathbf{x}) \nabla u) + \eta \left(u + av - cuv - uv^2 \right),$$
$$\frac{\partial v}{\partial t} = \nabla \cdot (\mathcal{D}_{22}(\mathbf{x}) \nabla v) + \eta \left(bv + hu + cuv + uv^2 \right),$$

$$\mathcal{D}_{11}(\mathbf{x}) \nabla u \cdot \mathbf{n} = 0, \quad \text{and} \quad \mathcal{D}_{22}(\mathbf{x}) \nabla v \cdot \mathbf{n} = 0.$$

For $\mathcal{D}(\mathbf{x})$ it is proposed:

$$\mathcal{D}(x,y) = \begin{pmatrix} \begin{pmatrix} 1-x^2 & 0 \\ 0 & 1-y^2 \end{pmatrix} & 0 \\ 0 & \begin{pmatrix} 1-x^2 & 0 \\ 0 & 1-y^2 \end{pmatrix} \end{pmatrix}.$$

With this, the spectral problem becomes:

$$\frac{\partial}{\partial x}\left(\left(1-x^2\right)\frac{\partial \Phi_1}{\partial x}\right)+\frac{\partial}{\partial y}\left(\left(1-y^2\right)\frac{\partial \Phi_1}{\partial y}\right)=-\rho\Phi_1,$$
$$\frac{\partial}{\partial x}\left(\left(1-x^2\right)\frac{\partial \Phi_2}{\partial x}\right)+\frac{\partial}{\partial y}\left(\left(1-y^2\right)\frac{\partial \Phi_2}{\partial y}\right)=-\rho\Phi_2,$$

with solution:

$$\Phi_m=\Phi_{ij}(x,y)=P_i(x)P_j(y),$$

where $m=1,2$, and eigenvalues

$$\rho=k_{ij}=i(i+1)+j(j+1).$$

A graphical interpretation of $\mathcal{D}(x, y)$ is given in a plot of $(1 - x^2) - (1 - y^2)$:

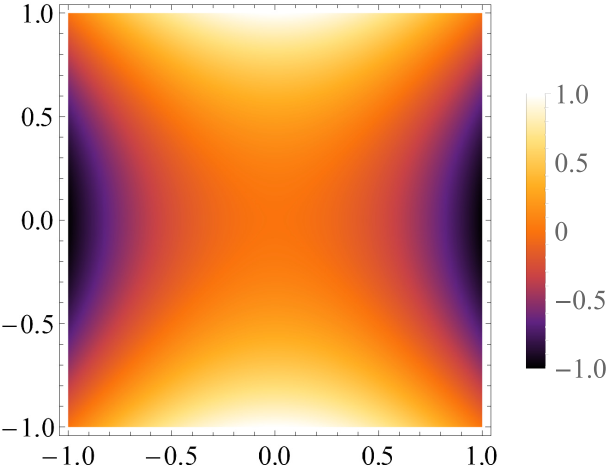

Similar to the case of homogeneous diffusion, after Taylor expanding F of the general non-homogeneous diffusion problem, we obtain:

$$\hat{w}\frac{\partial \hat{\mathbf{u}}}{\partial T} = D\nabla \cdot \mathcal{D}(\mathbf{x})\nabla \hat{\mathbf{u}} + \eta J\hat{\mathbf{u}} + Q(\hat{\mathbf{u}}, \hat{\mathbf{u}}) + C(\hat{\mathbf{u}}, \hat{\mathbf{u}}, \hat{\mathbf{u}}) + \cdots .$$

The perturbation method produces:

$$\begin{aligned}
\mathrm{O}(\epsilon): &\quad \mathcal{L}\mathbf{u}_1 = \mathbf{0},\\
\mathrm{O}(\epsilon^2): &\quad \mathcal{L}\mathbf{u}_2 = \mathbb{Q}(\mathbf{u}_1, \mathbf{u}_1) + p_1\eta\mathbb{J}_p^c\mathbf{u}_1 - w_1\frac{\partial \mathbf{u}_1}{\partial T},\\
\mathrm{O}(\epsilon^3): &\quad \mathcal{L}\mathbf{u}_3 = \mathbb{Q}(\mathbf{u}_1, \mathbf{u}_2) + \mathbb{C}(\mathbf{u}_1, \mathbf{u}_1, \mathbf{u}_1) + p_2\eta\mathbb{J}_p^c\mathbf{u}_1 + p_1\eta\mathbb{J}_p^c\mathbf{u}_2 +\\
&\qquad p_1\mathbb{Q}^c(\mathbf{u}_1, \mathbf{u}_1) - w_1\frac{\partial \mathbf{u}_2}{\partial T} - w_2\frac{\partial \mathbf{u}_1}{\partial T},
\end{aligned}$$

but now $\mathcal{L} = (-\eta\mathbb{J} - \mathbb{D}\nabla \cdot (\mathcal{D}(x, y)\nabla))$.

Now, we follow the same procedure as for the case of homogeneous diffusion but using the eigenfunctions $P_k(x)$ and $P_k(y)$, instead of $e^{i\mathbf{k}\cdot\mathbf{x}}$.

For example, the solution of $O(\epsilon)$ is proposed as linear combination of two spatial modes:

$$\mathbf{u}_1 = \mathbf{V}^{(1)} a(T) P_{i_c}(x) + \bar{\mathbf{V}}^{(1)} \bar{a}(T) P_{j_c}(y),$$

where $k_{i_c j_c}$ satisfies the diffusion-driven instability conditions.

In all that follows, we need the following:

$$P_k^2 = \sum_{n=0}^{2k} \xi_n P_n, \quad P_k P_m = \sum_{n}^{q+m} \zeta_n P_n, \quad P_k^3 = \sum_{n}^{3k} \chi_n P_n,$$

J. Dougall, *Proc. Glasg. Math. Assn.* **3** (1953) 121.

By following the above procedure, we are able to find the coefficients of the Stuart-Landau amplitude equations:

$$E = \frac{1}{2}\left\langle \mathbf{V}^* \middle| \mathbf{V}^{(1)} \right\rangle,$$

$$\alpha = \frac{1}{E}\left\langle \mathbf{V}^* \middle| \sum_{s=i_c+1}^{2i_c} Q(\mathbf{V}^{(1)}, \mathbf{V}_s^{(2)})\zeta_{i_c}^{(s)} + (\mathbf{V}^{(1)}, \mathbf{V}^{(1)})\chi_{i_c} \right\rangle,$$

$$\beta = \frac{1}{E}\left\langle \mathbf{V}^* \middle| Q(\bar{\mathbf{V}}^{(1)}, \mathbf{V}_{ij})\xi_0 + Q(\mathbf{V}^{(1)}, \bar{\mathbf{V}}_0^{(2)}) + 3C(\bar{\mathbf{V}}^{(1)}, \mathbf{V}^{(1)})\xi_0 \right\rangle,$$

$$\theta = \frac{1}{E}\left\langle \mathbf{V}^* \middle| p_2 \eta J_p^c \mathbf{V}^{(1)} \right\rangle.$$

Calderón-Barreto, Aragón, *Chaos. Sol. Frac.* **165** (2022) 112869.

Nonlinear analysis

With these coefficients, the conditions for the formation of stripes or spots can be determined.

For the VBAM model:

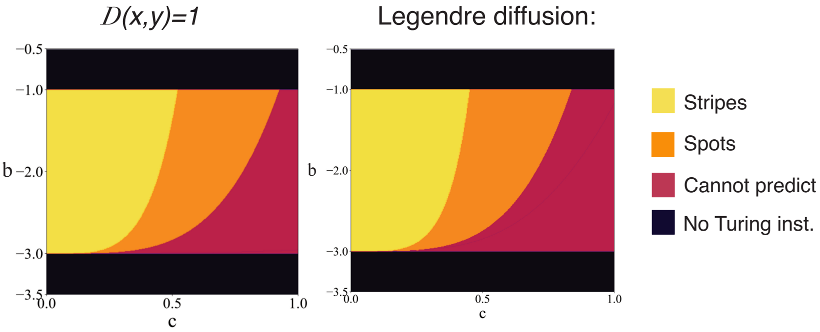

$a = 3, \; h = -1$

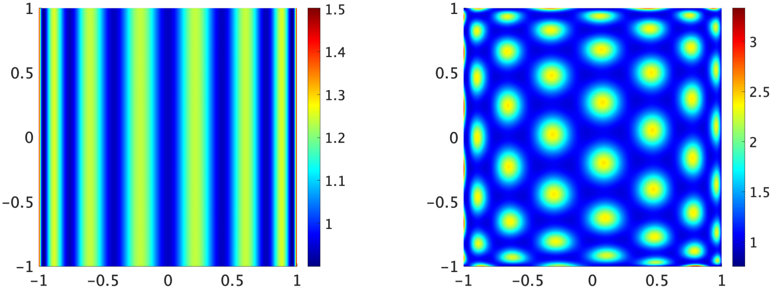

Stripes: $(c, b) = (0.01, -2.5)$

Spots: $(c, b) = (0.5, -2.5)$

$d_c = 0.1681$, $k_c = 14$, and $\eta = 121.757$

Jacobi

$$\mathcal{D}(x) = (1-x)^{1+\alpha}(1+x)^{1+\beta}$$

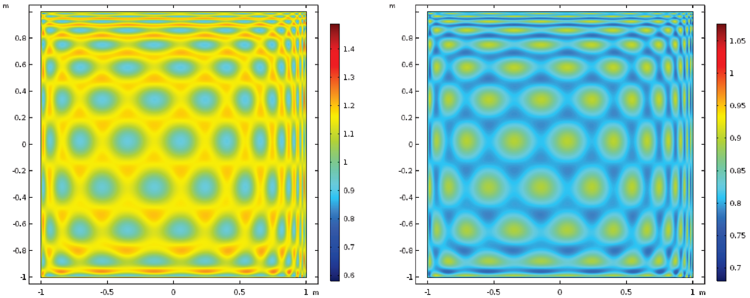

Hermite

$$\mathcal{D}(r) = \cos\left(\frac{\pi}{2} r\right)^2 e^{-\tan\left(\frac{\pi}{2} r\right)^2}$$

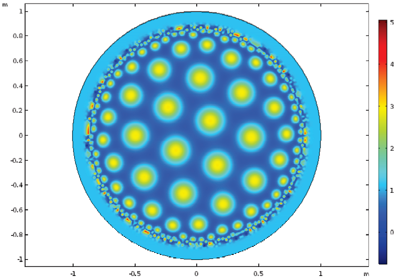

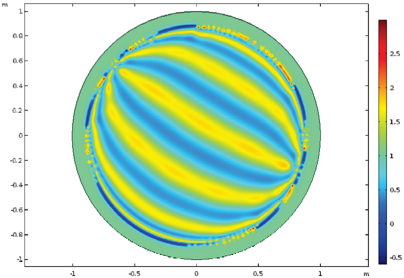

Conclusions

- By studying a particular case of the space-dependent diffusion coefficient, we propose a novel generalization of the standard weakly nonlinear analysis using Legendre functions instead of the standard Fourier approach.
- Our approach can motivate further generalization by using orthogonal eigenfunctions of any Sturm-Liouville problem.
- Our results can also be of interest in other fields such as climate modeling. Interestingly, in variants of the well studied Budyko-Seller climate model the time-dependent energy balance equation has the spatial operator $\frac{d}{dx}\left(k(1-x^2)\frac{du}{dx}\right)$.

Obrigado !